

## Introduction

The  $X_{cJ}(1P)$  states (with  $J = 0, 1, 2$ ) are the only triplet of P-wave states below the open-charm threshold. The hyperfine mass splitting is small and the branching fractions are 1.3%, 34.4% and 19.5% respectively. The  $X_{cJ}$  may be produced directly in pp collisions or through the decay of higher mass quarkonium states (prompt); or through the decay chains of b-hadrons (non-prompt). This analysis presents the measurement of the inclusive production of the  $X_{c1}$  and  $X_{c2}$  states in LHC pp collision at 7 TeV with the ATLAS detector.

## Data and Monte Carlo Samples

The data sample corresponds to an integrated luminosity of  $4.5 \text{ fb}^{-1}$  collected during the 2011 LHC pp run at a  $\sqrt{s} = 7 \text{ TeV}$ . Four Monte Carlo samples ( $X_{c1} \rightarrow J/\psi \rightarrow \mu^+ \mu^- \gamma$  and  $X_{c2} \rightarrow J/\psi \rightarrow \mu^+ \mu^- \gamma$ ) produced either directly or through the process  $pp \rightarrow b\bar{b}X \rightarrow X_{cJ}$  are used to estimate the photon conversion reconstruction efficiency and to characterize the modeling of the  $X_{cJ}$  signal components. All samples are generated with PYTHIA6 and use the ATLAS 2011 MC underlying event and hadronization model tuning. The detector response is simulated using GEANT4.

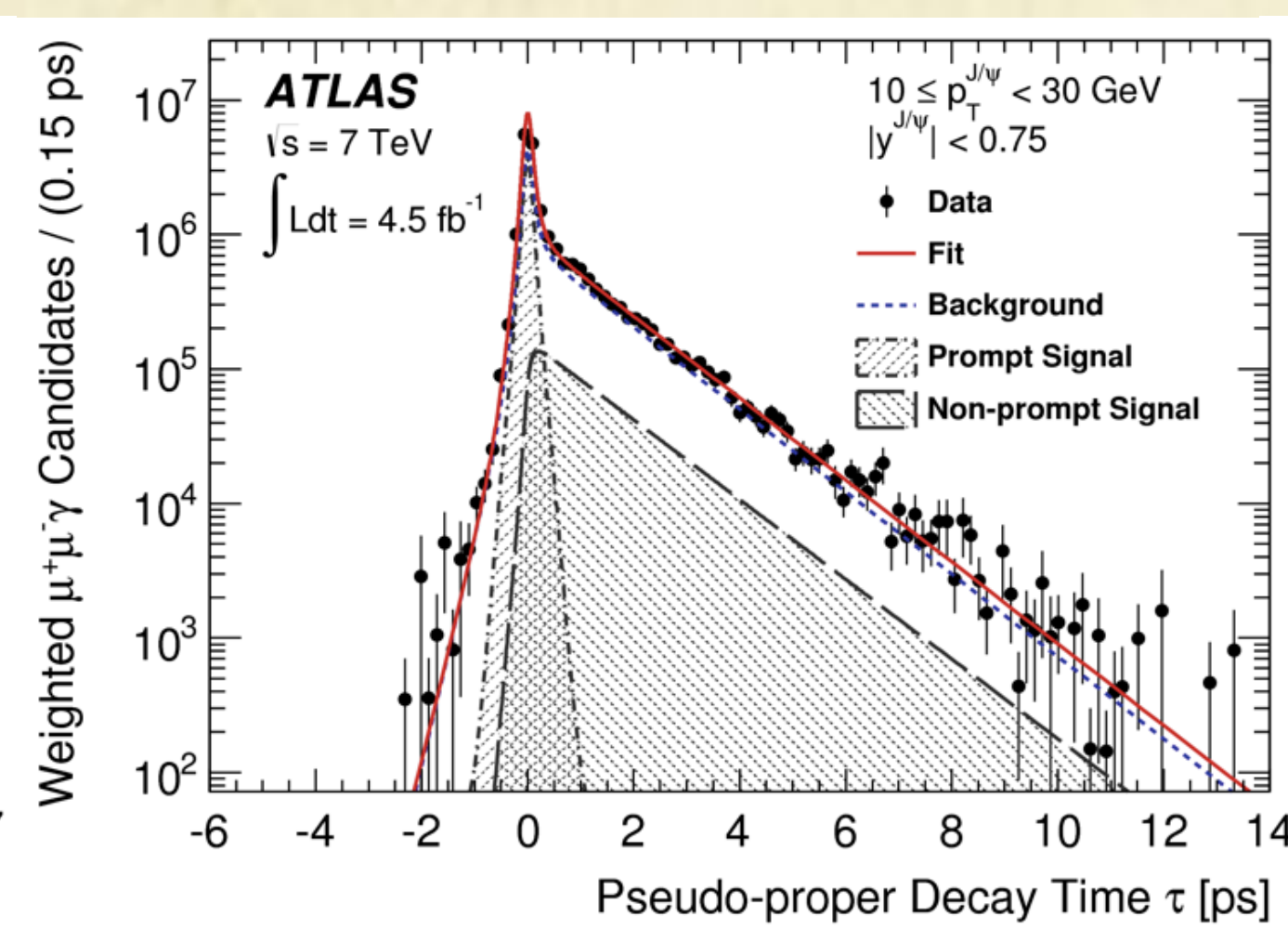
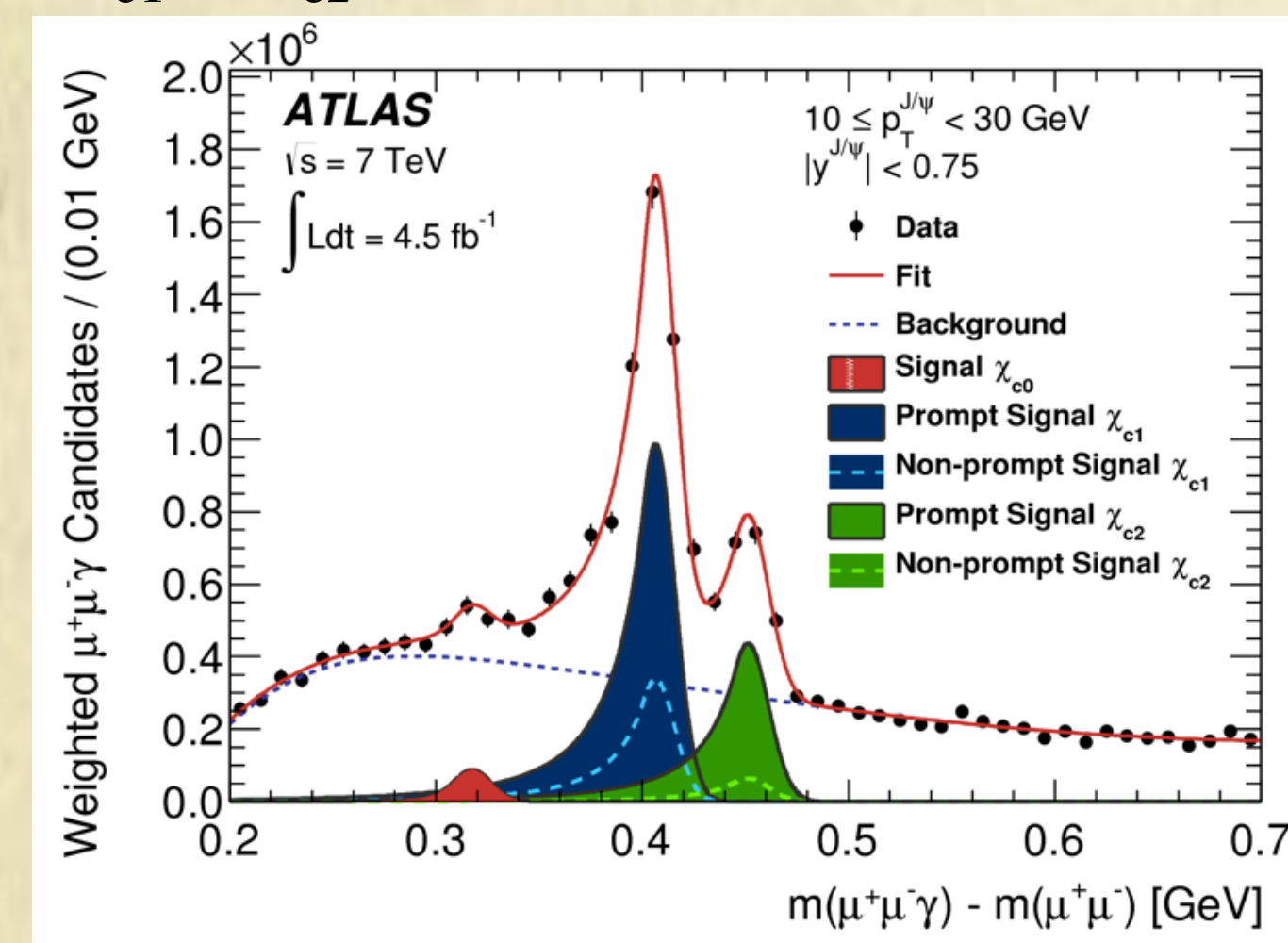
## Event and $X_c$ Candidate Selection

Event selection  $X_c \rightarrow J/\psi \gamma$ :  
Di-muon trigger:  $p_T > 4 \text{ GeV}$ ;  $2.5 < m_{\mu\mu} < 4.0 \text{ GeV}$ ; at least 1 pp collision vertex with at least 3 tracks with  $p_T > 400 \text{ MeV}$   
 $J/\psi$ :  $p_T^\mu > 4 \text{ GeV}$ ;  $|\eta^\mu| < 2.3$ ;  $2.95 < m_{\mu\mu} < 3.25 \text{ GeV}$ ;  $|y^{J/\psi}| < 0.75$   
Converted photon: oppositely charged track pairs  $p_T > 400 \text{ MeV}$ ;  $|\eta| < 2.3$ ;  $40 < r(\text{pair}) < 150 \text{ mm}$ ;  $p_T^\gamma > 1.5 \text{ GeV}$ ;  $|\eta^\gamma| < 2.0$   
 $X_c$ : associate candidates  $J/\psi$  and  $\gamma$ ; impact parameter of  $\gamma$  from di-muon vertex  $< 5$  to remove combinatorial bkg.

## Cross-Section Determination

$X_{c1}/X_{c2}$  separation variable:

Prompt/non prompt separation variable:



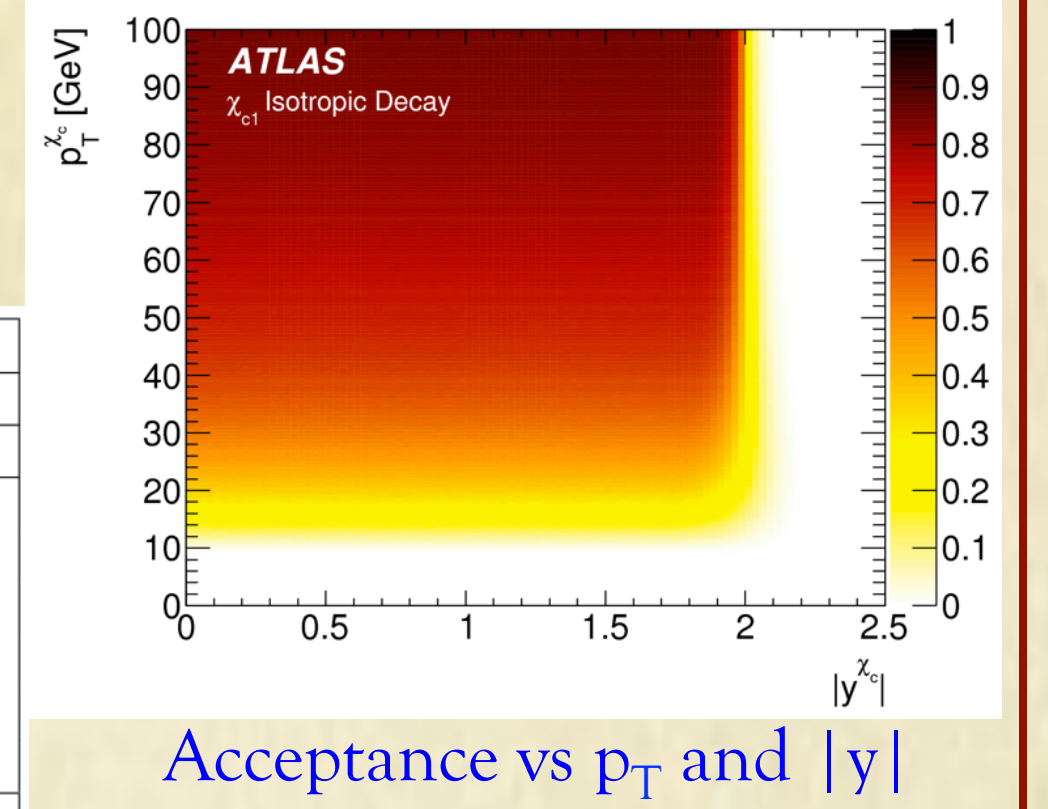
$$\tau = \frac{L_{xy} \cdot m_{J/\psi}}{|\vec{p}_T^{\gamma}|}$$

$$\frac{d\sigma(X_{cJ})}{dp_T^{X_c}} \cdot \mathcal{B}(X_{cJ} \rightarrow J/\psi \gamma) \cdot \mathcal{B}(J/\psi \rightarrow \mu^+ \mu^-) = \frac{N_J}{\mathcal{L} \cdot \Delta p_T^{X_c}}$$

$N_J$  = acceptance and efficiency corrected yield

Correction weight:  $w^{-1} = \mathcal{A} \cdot \epsilon_{\text{trig}} \cdot \epsilon_{\text{di-muon}} \cdot \epsilon_{\text{conv}}$

Binning: $p_T^{J/\psi}$	Fractional Uncertainty [%]				Binning: $p_T^{X_c}$	Fractional Uncertainty [%]			
	Prompt		Non-prompt			Prompt		Non-prompt	
Muon reco. efficiency	1	1	1	1	Muon reco. efficiency	1	1	1	1
Trigger efficiency	4	4	4	4	Trigger efficiency	3	4	4	4
Converted-photon reco. efficiency	11	11	11	11	Converted-photon reco. efficiency	11	11	11	11
Conversion probability	4	4	4	4	Conversion probability	4	4	4	4
Acceptance	4	4	5	8	Acceptance	2	2	2	2
Fit model	2	3	3	9	Fit model	2	3	3	8
Total systematic	13	13	13	17	Total systematic	12	12	12	14
Spin-alignment envelope (upper)	34	36	32	36	Spin-alignment envelope (upper)	29	31	29	31
Spin-alignment envelope (lower)	13	23	13	23	Spin-alignment envelope (lower)	11	20	11	20

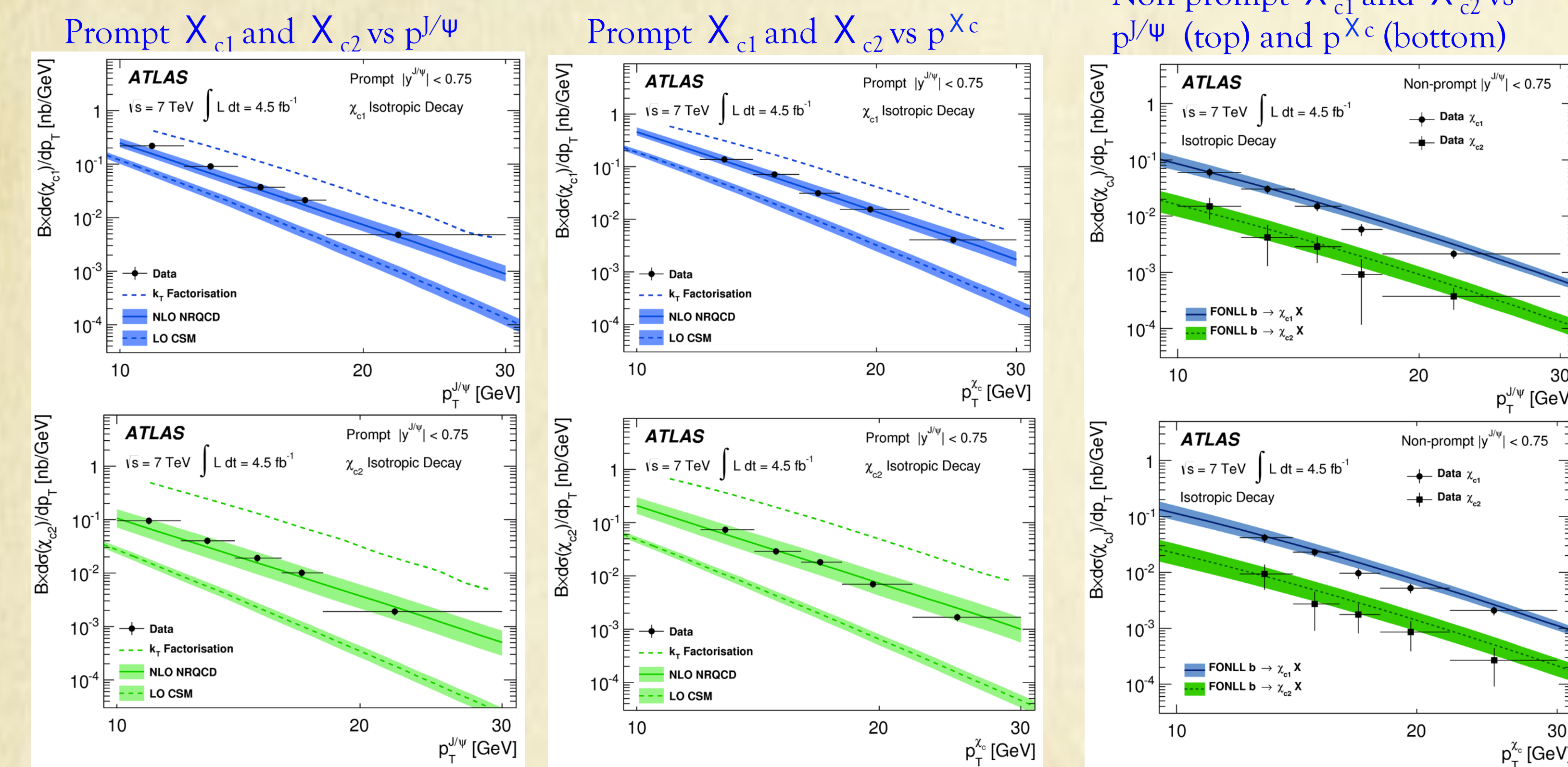


Corrected yields are extracted by performing a simultaneous fit to the mass difference and pseudo-proper time distributions of weighted  $X_c$  candidates. Probability Distribution Function used:

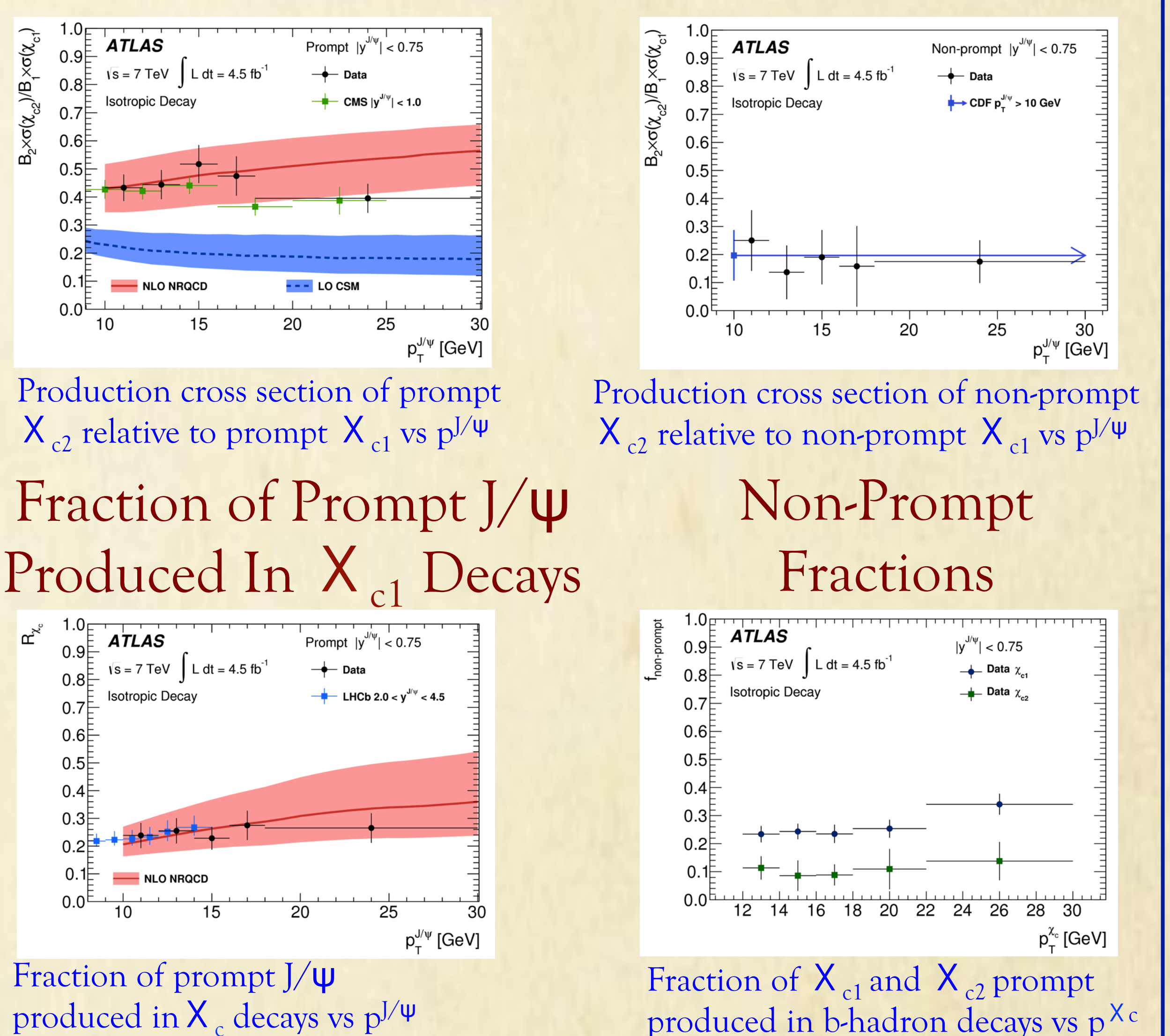
$$F(\Delta m, \tau, \delta\tau) = f_{\text{Sig}} \cdot F_{\text{Sig}}(\Delta m, \tau, \delta\tau) + (1 - f_{\text{Sig}}) \cdot F_{\text{Bkgd}}(\Delta m, \tau, \delta\tau)$$

Contributions to the total uncertainty on the cross section measurements binned in  $p^{J/\psi}$  ( $p^{X_c}$ ) averaged across all  $p^{J/\psi}$  ( $p^{X_c}$ ) bins. Contributions of integrated luminosity (1.8%) and track reconstruction (1%) are not shown. The average variation in acceptance corresponding to all possible polarization scenarios is also shown.

## Differential Cross Sections



## Cross Section Ratios



## Measurement of $\text{Br}(B^\pm \rightarrow X_{c1} K^\pm)$

Relative measurement:  $B^\pm \rightarrow J/\psi K^\pm$  used as reference channel (same final state except of the photon)

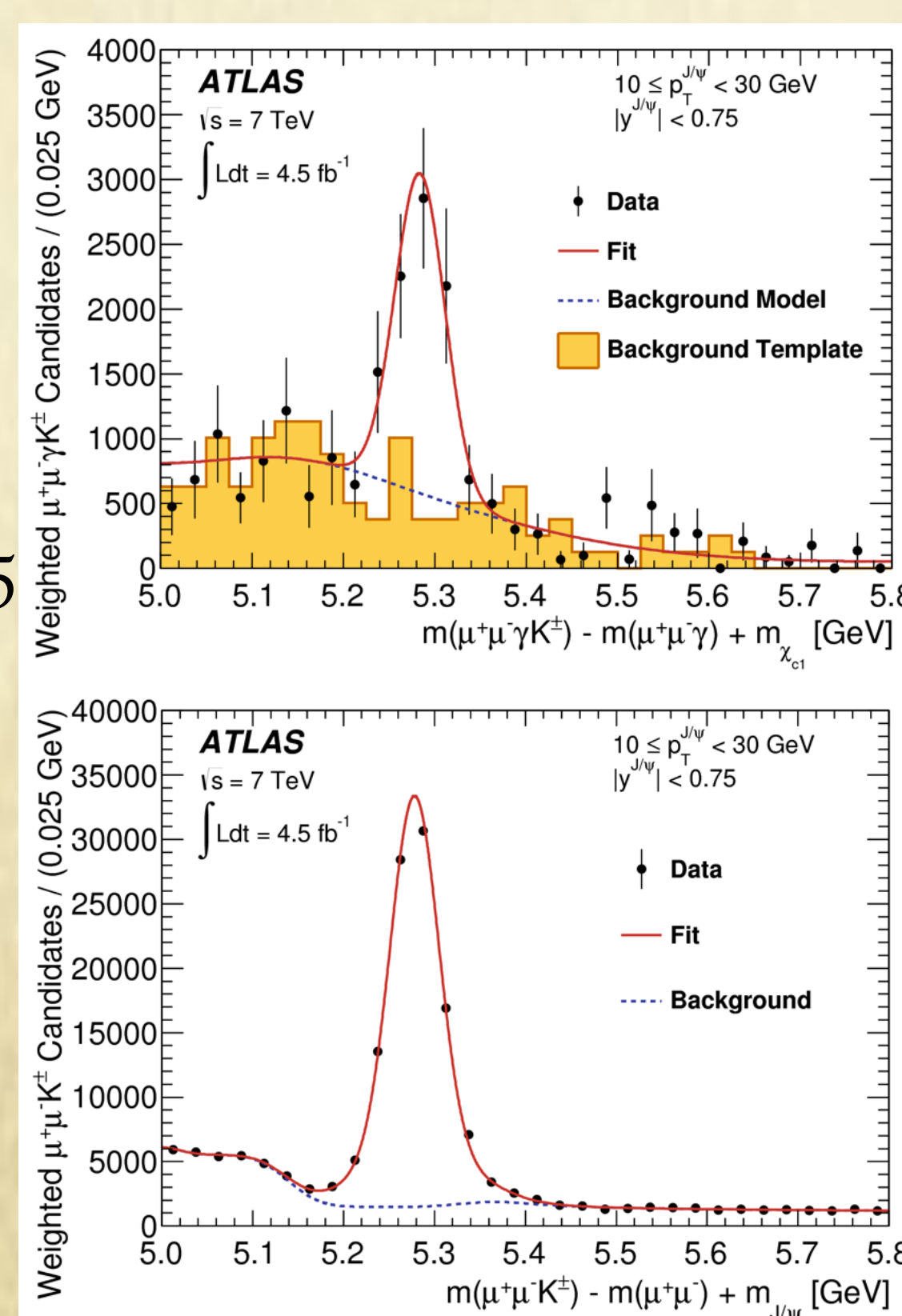
$$\mathcal{B}(B^\pm \rightarrow X_{c1} K^\pm) = \mathcal{A}_B \cdot \frac{N_{X_{c1}}^B}{N_{J/\psi}^B} \cdot \frac{\mathcal{B}(B^\pm \rightarrow J/\psi K^\pm)}{\mathcal{B}(X_{c1} \rightarrow J/\psi \gamma)}$$

$\text{Br}(B^\pm \rightarrow J/\psi K^\pm) = (1.016 \pm 0.033) \times 10^{-3}$ ;  $\text{Br}(X_{c1} \rightarrow J/\psi \gamma) = 0.344 \pm 0.015$   
Decays reconstructed in  $10 < p_T^{J/\psi} < 30 \text{ GeV}$ ;  $|y^{J/\psi}| < 0.75$   
Same data sample, and selection as the  $X_c$  analysis

	Fractional Uncertainty [%]
Converted-photon reconstruction efficiency	10
Conversion probability	4
Muon reconstruction efficiency	1
Trigger efficiency	1
Acceptance	3
Fit model	6
Statistical	18
Systematic	13
Total	22

$$\text{Br}(B^\pm \rightarrow X_{c1} K^\pm) = (4.8 \pm 0.6^{\text{stat}} \pm 0.6^{\text{syst}}) \times 10^{-4}$$

Good agreement with PDG value  $(4.9 \pm 0.23) \times 10^{-4}$



## Conclusions

The cross sections for prompt and non-prompt  $X_{c1}$  and  $X_{c2}$  production have been measured in pp collisions at  $\sqrt{s} = 7 \text{ TeV}$  with the ATLAS detector at the LHC. Production rate of the  $X_{c2}$  state is measured relative to the  $X_{c1}$  state for both prompt and non-prompt production as a function of  $p_T^{J/\psi}$ . The fraction of prompt  $J/\psi$  produced in feed-down from  $X_c$  decays is also derived. The fractions of  $X_{c1}$  and  $X_{c2}$  produced in the decays of b-hadrons are also presented as functions of  $p_T^{X_c}$ . Finally, the branching fraction  $\text{Br}(B^\pm \rightarrow X_{c1} K^\pm) = (4.8 \pm 0.6^{\text{stat}} \pm 0.6^{\text{syst}}) \times 10^{-4}$  is measured with the same dataset and  $X_c$  event selection.